ORAL/POSTER REFERENCE: ICF100579OR

CRACK GROWTH IN SOLID PROPELLANTS

E.E. Gdoutos and G. Papakaliatakis

School of Engineering, Democritus University of Thrace
GR-671 00 Xanthi, Greece

ABSTRACT

An analytical investigation of the growth behavior of an edge crack in a rectangular sheet specimen made of a solid propellant was performed. The specimen was subjected to a uniform displacement along its upper and lower faces. The solid propellant was simulated as a hyperelastic material with constitutive behavior described by the Ogden strain energy potential. A nonlinear finite deformation analysis of the stress and displacement fields was performed using the finite element code ABAQUS. A very detailed analysis of the stress field in the vicinity of the crack tip was undertaken. The deformed profiles of the crack faces near the crack tip were determined. The results of stress analysis were coupled with the strain energy density theory to predict the crack growth behavior including crack initiation, stable crack growth and final termination. Crack growth resistance curves representing the variation of crack growth increments versus applied displacement were drawn.

KEYWORDS

Crack growth, Solid propellant, Finite element analysis, Hyperelastic material, Nonlinear behavior, Finite deformations.

INTRODUCTION

Solid propellants are particulate composite materials, containing hard particles embedded in a rubber matrix. On the microscopic scale, a highly filled propellant can be considered as nonhomogeneous. When the material is strained, damage in the form of microvoids in the binder or debonding at the matrix/particle interface takes place. As the applied strain in the material is progressively increased the growth of damage takes place as successive nucleation and coalescence of the microvoids or as material tears. These processes of damage initiation and evolution are time-dependent and they are mainly responsible for the time-sensitivity of the nonlinear stress-strain behavior of solid propellants. Their mechanical response is strongly influenced by the loading rate, temperature and material microstructure.

A considerable amount of work has been performed by Liu and coworkers [1-3] to study crack growth behavior in solid propellants. They investigated the characteristics of damage zone near the crack tip and crack growth behavior in cracked specimens of a solid propellant. From experimental results they established that the damage characteristics have strong effects on crack growth behavior. Crack growth consists of crack tip blunting, resharpening and zig-zag crack growth.
The objective of the present work is to study the characteristics of the damage zone near the crack tip and

the crack growth behavior in edge and centrally cracked sheet specimens of a solid propellant. The stress field in the cracked plates is evaluated by modeling the solid propellant as an incompressible visco-hyperelastic material. A very detailed finite element analysis in the vicinity of the crack tip takes place. A methodology based on the strain energy density criterion is developed for the determination of the critical stress at the onset of crack initiation and the history of stable crack growth up to final instability.

CONSTITUTIVE BEHAVIOR

Solid propellants are modeled as hyperelastic materials. The behavior of hyperelastic materials is described in terms of a strain energy potential U(ε). The more frequently used forms of the strain energy potentials for modeling approximately incompressible isotropic materials are the polynomial form and the Ogden form.

The form of the polynomial strain energy potential is

$$U = \sum_{i+j=1}^{N} C_{ij}(\bar{I}_1 - 3)^i(\bar{I}_2 - 3)^j + \sum_{i=1}^{N} \frac{1}{D_i}(J_{e\lambda} - 1)^{2i} \tag{1}$$

where U is the strain energy per unit of reference volume, N is a material parameter, C_{ij} and D_i are temperature dependent material parameters, $\bar{I}_1$ and $\bar{I}_2$ are the first and second deviatoric strain invariants, defined as

$$\bar{I}_1 = \bar{\lambda}_1^2 + \bar{\lambda}_2^2 + \bar{\lambda}_3^2 \quad and \quad \bar{I}_2 = \bar{\lambda}_1^{(-2)} + \bar{\lambda}_2^{(-2)} + \bar{\lambda}_3^{(-2)}$$

with the deviatoric stretches $\bar{\lambda}_i = J^{-1/3}\lambda_i$, J is the volume ratio, λ_i are the principal stretches, and J_{el} is the elastic volume ratio without thermal expansion effects.

The form of the Ogden strain energy potential is

$$U = \sum_{i=1}^{N} \frac{2\mu_i}{\alpha_i^2}\left(\bar{\lambda}_1^{a_i} + \bar{\lambda}_2^{a_i} + \bar{\lambda}_3^{a_i} - 3\right) + \sum_{i=1}^{N} \frac{1}{D_i}(J_{e\lambda} - 1)^{2i} \tag{2}$$

N is a material parameter, and μ_i, α_i and D_i are temperature dependent material parameters. Because the powers α_i can be chosen by the user, the Ogden form usually provides a closer and more stable fit to the test data for a similar number of material constants in the strain energy function, especially at large strains. If all of the D_i are zero, the material is fully incompressible. If D_1 is equal to zero, all of the D_i must be equal to zero.

For cases where the nominal strains are small or only moderately large (<100%), the first terms in the polynomial series usually provide a sufficiently accurate model. The simplest form of the polynomial function is the form with N=1, which is the compressible form of the classical Mooney-Rivlin law:

$$U = C_{10}(\bar{I}_1 - 3) + C_{01}(\bar{I}_2 - 3) + \frac{1}{D_1}\left(J_{e\lambda} - 1\right)^2 \tag{3}$$

When C_{01}=0 the strain energy function corresponds to the compressible form of the neo-Hookean law.

FINITE ELEMENT ANALYSIS

The finite element method was used to solve the boundary value problem of an edge cracked specimen subjected to a uniform displacement along its upper and lower faces. The specimen is a rectangular sheet of width w=76.2 mm and height h=25.4 mm (Fig. 1). The thickness of the specimen was small enough to assume that conditions of plane stress prevail. An initial edge crack was introduced in the mid height of the specimen parallel to the specimen width. The crack length took the values a=2.54 mm, 15.24 mm and 30.48 mm. The specimen was made of a solid propellant. It was subjected to a uniform displacement u_0 along its upper and lower faces. The stress-strain curve of the propellant in tension is shown in Fig. 2.

A nonlinear large deformation analysis was performed by the ABQUS computer code. The discretization of a small region of the specimen crack tip are presented in Fig. 3. The applied displacement u_0 was increased incrementally. Results for the strain energy density, dW/dV, along the crack axis direction, are shown, in Fig. 4 for a=15.24 mm and for applied displacement u=0.0847 mm, 0.1694 mm and 0.2541 mm.

PREDICTION OF CRACK GROWTH

Crack growth consists of three stages: crack initiation, subcritical or slow growth and unstable crack propagation. These stages of crack growth will be addressed in a unified manner by the strain energy density criterion. The criterion was introduced by Sih , and it was used by Gdoutos and co-workers [4-6] for the solution of a host of problems of engineering importance.According to the strain energy density theory crack growth takes place when the strain energy density at an element ahead of the crack tip reaches a critical value. This value is calculated from the stress-strain curve of the material in tension.

$$\frac{dW}{dV} = \int_0^{\varepsilon_{ij}} \sigma_{ij} d\varepsilon_{ij} \tag{4}$$

where σ_{ij} and ε_{ij} are the Cartesian stress and strain components. Equation (1) applies to all materials either linear (nondissipative) or nonlinear (dissipative).For the case when material failure initiates from the tip of a preexisting crack in a solid propellant attention is concretrated on the distribution of the strain energy function along the circumference of a circle centered at the crack tip. This circle represents the process or core region in which the continuum model fails to describe the state of stress and strain. The crack will grow in the direction of the minimum strain energy density function, $(dW/dV)_{min}$. Onset of crack extension takes place when $(dW/dV)_{min}$ becomes equal to $(dW/dV)^c_{min}$ (referred to in sequel as $(dW/dV)_c$) which is directly determined from the area underneath the stress-strain diagram of the material up to the point of fracture. Crack growth initiation is expressed by

$$\left(\frac{dW}{dV}\right)_{min} = \left(\frac{dW}{dV}\right)_c \tag{5}$$

where $(dW/dV)_c$ is a material parameter.The value of the critical stress σ_i that triggers crack growth is determined from equation (5). The condition for stable crack growth is expressed by

$$\frac{dW}{dV} = \left(\frac{dW}{dV}\right)_c = \frac{S_1}{r_1} = \frac{S_2}{r_2} = \ldots = \frac{S_j}{r_j} = \ldots \frac{S_c}{r_c} \tag{6}$$

where r_m (m=1,2,...,j) are the crack growth increments. Crack growth becomes unstable when the critical crack increment r_c is reached. r_c is a material parameter and is calculated from $r_c=S_c/(dW/dV)_c$, where S_c is material parameter.The graphical procedure for the determination of the critical applied displacement u

for initiate of crack growth are presented in Fig. 4 for a crack length a=15.24 mm. In this figure r_0 is the radius of the core region within which the continuum model ceases to be able to represent the state of stress and strain. For analysis purposes in the present study r_0 was taken equal to r_0=0.014 mm. Based on the strain energy density criterion a series of crack growth increments are determined until the crack growth increment reaches the critical value r_c=1.6 mm. The R-curve for this case is shown in Fig. 5. The deformed profile of the crack face near the crack tip for applied displacement u=0.4235, 1.2705, 2.1175 and 2.9645 mm is shown in Fig. 6. Results for the critical stress for crack initiation and growth for various crack lengths is shown in Fig. 7.

ACKNOWLEDGEMENTS

The authors express their appreciation to Dr. C.T. Liu of the USAF, Phillips Lab., Edwards AFB for his encouragement, support and cooperation during the course of the present work.

REFERENCES

1. Liu, C.T. (1995) *J. Spacecrafts and Rock.* 32, 535.
2. Liu, C.T. (1992) *J. Spacecrafts and Rock.* 29, 713.
3. Liu, C.T. and Tang, B. (1995). *Proc. 1995 SEM Spring Conf.,* pp. 831-836.
4. Gdoutos, E.E. and Papakaliatiakis, G. (1986) *Ther. Appl. Fract. Mech.* 5, 133.
5. Gdoutos, E.E. and Papakaliatiakis, G. (1986) *Int. J. Fract.* 32, 143.
6. Gdoutos, E.E. and Papakaliatiakis, G. (1986) *Eng. Fract. Mech.* 25, 141.

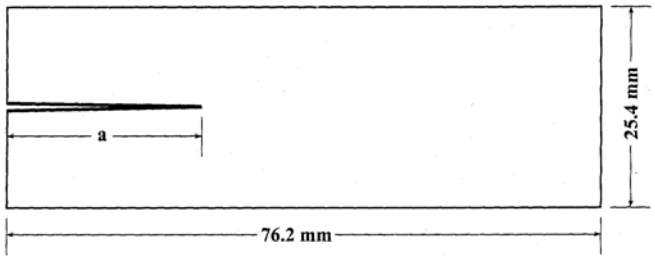

Fig. 1 Geometry of edge-cracked specimen

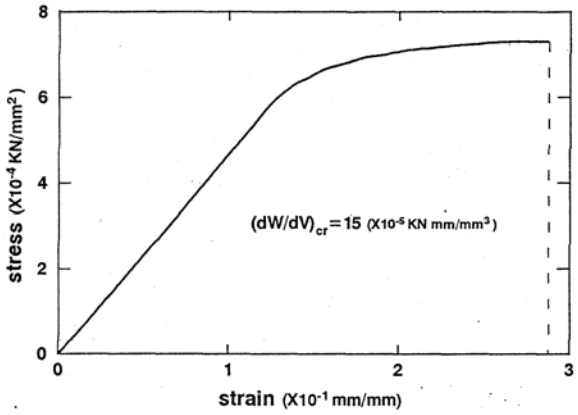

Fig. 2 Stress-strain curve of the solid propellant in uniaxial tension

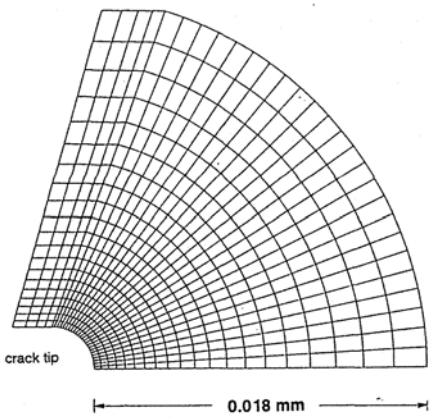

Fig. 3 Finite element grid pattern in a small region near the crack tip.

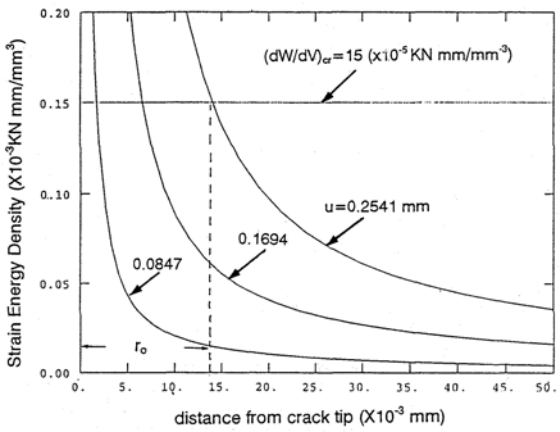

Fig. 4 Determination of the critical value of u at crack initiation

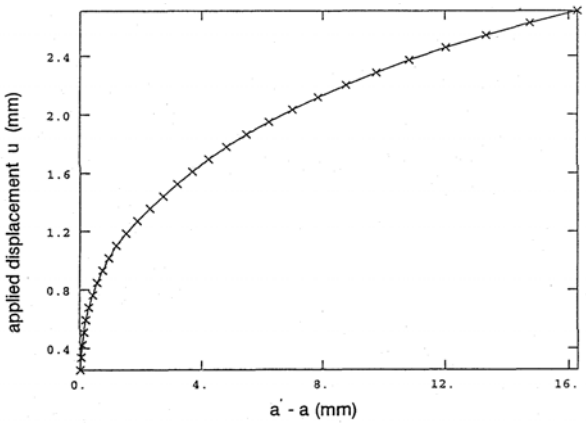

Fig. 5 Crack growth resistance curve.

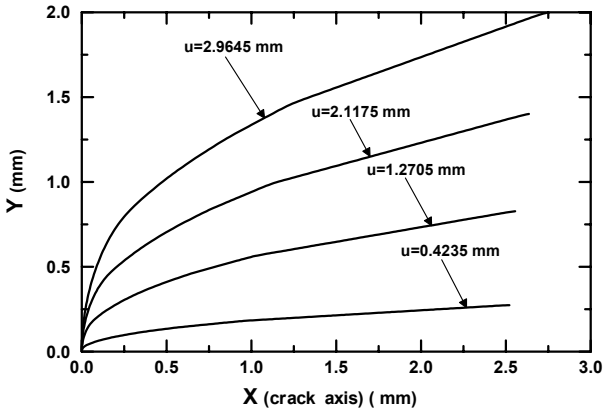

Fig. 6 Deformed profile of cracks faces near the crack tip for various values of the uniform applied displacement u.

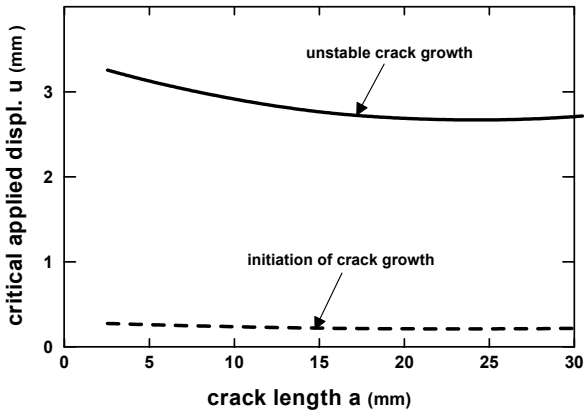

Fig. 7 Variation of the critical applied displacement u for crack initiation and unstable growth for various crack lengths